Experimental and theoretical study of the anisotropy induced in a gas laser by a saturating field

G. Stephan*
Institute of Physics, University of Oran, Algeria

R. Le Naour
Laboratoire d'Electronique Quantique, Université de Nantes, BP 1044, Nantes, 44037, France

A. Le Floch
Laboratoire d'Electronique Quantique, Université de Rennes, BP 25A, Rennes, 35031, France
(Received 28 February 1977)

The optical anisotropy induced by a saturating stationary field in a gas laser which is initially isotropic is described theoretically. The calculation of the polarizability tensor shows that linear or circular anisotropies can be induced depending upon the electromagnetic field polarization. The Jones matrix formalism is extended to the nonlinear case. The experimental verification of the predicted linear gain anisotropy in a He-Ne laser is obtained at 3.39 μm. The Jones matrix for a probe field in this particular case is also calculated. The corresponding linear anisotropy is attributed to Zeeman coherences between sublevels. Moreover, we find that the maximum of this anisotropy is slightly shifted from the center of the line.

I. INTRODUCTION

Lamb's theory of the laser[1] has been successfully used to explain many experimental results such as the Lamb dip, mode-coupling effects and related phenomena. This theory works particularly well for scalar phenomena. The model includes two parts: an active one (the amplifying gas) and a passive one (the resonant cavity). Lamb introduced the latter as a loss distributed in the former. The field in the laser then obeys a Maxwell equation in which one includes a term that accounts phenomenologically for attenuation. The different optical devices in the cavity are then delocalized (i.e., they are assumed to be uniformly distributed) and the equation mentioned above describes only a "mean" field. These optical devices are mirrors, windows, or Faraday rotators, for example. However, the Lamb model does not permit the study of the variations of the electromagnetic (e.m.) field along the axis of the laser. Yet these variations exist: it has been already shown[2] that, at a point, the two progressive waves constituting a stationary mode can have two different polarizations and that these polarizations can vary in the laser. This effect can be explained using the spatial vectorial theory based on the resonance condition. In this theory, each optical component of the cavity is localized and represented by a Jones matrix.[3] The light goes back and forth in the laser and is transformed by these components. In a stationary state, the electric vector is one of the eigenvectors of the appropriate products of Jones matrices; after a round trip in the cavity this vector remains unchanged. This is called the resonance condition.

We have used this method[2] and have experimentally verified its results in the case of cavities containing linear-loss,[4,5] linear-phase,[6] and circular-phase[7] anisotropies. However, in these papers, it was supposed that for monomode lasers the anisotropies of the amplifying medium[8] were weak and could be neglected. It was sufficient to know the Jones matrices of the optical components in order to solve the problem of determining the stationary state.

This approximation is very good in the case where the polarizations of the two counter-propagating waves in the amplifying gas coincide. If this is not the case, there may be anisotropies of the optical components which are of the same order of magnitude as those induced in the amplifying medium by the field. A competition could arise and determining the field would then become a complicated self-consistency problem. The aim of the present paper is to provide an introduction to that kind of problem by defining and calculating the Jones matrix of the saturated "atoms + field" system.

The level degeneracy is shown to give rise to anisotropies. Its importance has already been shown by Doyle and White[9] but only in the case of coupling between two modes with different frequencies in the laser. An indirect study of the induced anisotropy in a vanishing magnetic field has been done experimentally by Delang and Bouwhuis[10] and theoretically analyzed by Van Haeringen.[11] However, experiments were done using a sealed laser with unknown cavity anisotropies so that

separation between the two kinds of anisotropies could not be achieved. Dienes[12] has studied the variation of the ellipticity of a wave propagating in an amplifying medium. Im. Thek-De *et al.*[13] and Yu. A. Vdovin *et al.*[14] have observed the interactions of two waves with different and tunable frequencies for various polarizations in an absorbing or amplifying medium. However, the saturated absorption experiment done by Shank and Schwarz[15] is closer to the spirit of our study. They used two progressive waves with identical but not variable frequency. The resonance condition has also been used by other authors in order to explain discrepancies[16a] with the distributed-loss Zeeman laser theory[1] and to describe some specific experimental results.[16b]

In Sec. II, it will be shown that the saturating field of the laser generally induces anisotropies in the gas and that the propagation matrix depends on two different atomic quantities: populations of the sublevels (scalar quantity) and Zeeman coherences (tensor quantity describing alignment). The second gives rise, in particular, to the linear anisotropy. In Sec. III we describe an experimental device designed to verify this effect. The laser field is linearly polarized, the "atoms + field" medium exhibits a linear anisotropy and behaves as an amplifying uniaxial crystal. To show the effect, we use a small linearly polarized probe field whose plane of polarization is rotated to permit a phase detection. We then find that the probe is more amplified when its polarization is perpendicular to that of the laser field. Furthermore, the experimental result shows an unexpected effect indicating that the maximum of this anisotropy is not at the center of the line.

II. THE PROPAGATION MATRIX

A. Hypothesis

The physical system we are interested in is an atomic gas interacting with a saturating e.m. field. We have in mind the weak gain active column of a single-mode TEM_{00} He-Ne laser in which the field $\vec{E}_{(z,t)}$ results from the composition of two progressive waves having approximately the same amplitude. Moreover, we suppose that the polarizations of these waves are different, and we write

$$\vec{E}_{(z,t)} = \vec{E}_1 e^{-i(\omega t - kz)} + \vec{E}_2 e^{-i(\omega t + kz)} + \text{c.c.}, \tag{1}$$

where ω is the angular frequency, k the wave vector, and z is measured along the axis of the laser. $\vec{E}_1$ and $\vec{E}_2$ represent amplitude and polarization of the two waves. Moreover, we suppose E_1 and E_2 to be complex in order that we may introduce a phase factor. The expression (1) is written at the point z; it is good only for a slice $dz \ll \lambda$ where λ is the wavelength. We attribute the same k to the two progressive waves because we suppose $|\vec{E}_1| \approx |\vec{E}_2|$. We write in the general case,

$$\vec{E}_1 = \mathcal{E}_1\hat{x} + e_1\hat{y}, \quad \vec{E}_2 = \mathcal{E}_2\hat{x} + e_2\hat{y}, \tag{2}$$

where $\hat{x}$ and $\hat{y}$ are unit vectors and $\vec{0x}, \vec{0y}, \vec{0z}$ define a right-handed Cartesian system [Fig. 1(a)]. One should notice that $\vec{E}_1$ and $\vec{E}_2$ can describe the fields outside or inside a cavity. However, in the latter case the two fields are not independent due to the resonance condition.[2] We take $\vec{0z}$ as the quantization axis. This is justified by the fact that $\vec{E}_1$ and $\vec{E}_2$ can have a general polarization which leaves only the propagation axis $\vec{0z}$ as a symmetry axis. Under these conditions the light beam $\vec{E}_1$ with polarization $\vec{\sigma}^+$ for instance would be written

$$\vec{E}_1 = \mathcal{E}(\hat{x} + i\hat{y}). \tag{3}$$

We then describe the atomic gas in the conventional manner[17] and consider only two-levels atoms [Fig. 1(b)]. The standard state vectors are $|a,m\rangle$ and $|b,m\rangle$. J_b and J_a are the angular momenta for upper (b) and lower (a) levels, and m is the magnetic quantum number. The eigenvalues of the nonperturbed Hamiltonian for the a and b levels are E_a and E_b with $E_a < E_b$ and $E_b - E_a = \hbar\omega_{ab}$. The system is described by a density operator $\rho_{(z,t)}$ and the polarization of the "atoms + field" system for the slice dz can be written

$$\begin{aligned}\vec{\mathcal{P}}_{(z,t)} &= \mathrm{Tr}(\rho_{(z,t)}\vec{\mu}) \\ &= \int_{-\infty}^{+\infty} dv \sum_m [\rho_{b_{m+1}a_m}(v,z,t)\vec{\mu}_{a_m b_{m+1}} \\ &\quad + \rho_{b_{m-1}a_m}(v,z,t)\vec{\mu}_{a_m b_{m-1}}] + \text{c.c.},\end{aligned} \tag{4}$$

where $\rho_{b_{m+1}a_m}(v,z,t)$ is the density matrix element between the sublevels b_{m+1} and a_m for the class of

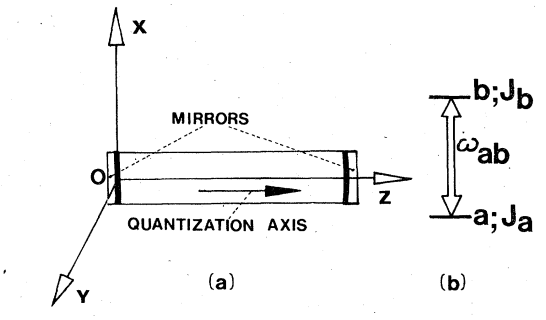

FIG. 1. (a) Definition of coordinate axes. The origin 0 coincides with one end of the active medium. (b) Two degenerate energy levels a and b having a resonance frequency ω_{ab} and angular momenta J_a and J_b.

atoms having the velocity v along the $\vec{0}z$ axis. $\vec{\mu}$ is the electric dipole operator and its matrix elements obey the selection rule $\Delta m = \pm 1$ because $\vec{0}z$ is used as the quantization axis. The polarizability tensor, the optical constants and the propagation matrix will then be deduced from $\vec{\mathcal{P}}_{(z,t)}$.

B. Calculation of the polarizability tensor

We must first calculate the matrix $\rho(v,z,t)$. For this purpose we use the evolution equation in the laboratory frame[18]

$$\left(\frac{\partial}{\partial t}+v\frac{\partial}{\partial z}\right)\rho(v,z,t) = \left(\frac{d}{dt}\rho(v,z,t)\right)_{\text{exc}+\text{relax}} - \frac{i}{\hbar}[\mathcal{H}_{(z,t)},\rho(v,z,t)]. \tag{5}$$

The Hamiltonian

$$\mathcal{H}_{(z,t)} = \mathcal{H}_0 - \vec{\mu}\cdot\vec{E}_{(z,t)} \tag{6}$$

contains the nonperturbed Hamiltonian $\mathcal{H}_0$ and the perturbation energy $-\vec{\mu}\cdot\vec{E}_{(z,t)}$ coupling the atom and the field in the electric dipole approximation. $\mathcal{H}_0$ is diagonal in the standard base and recoil effects are neglected. We simplify the problem in making *ad hoc* assumptions on the excitation-relaxation term $[d\rho(v,z,t)/dt]_{\text{exc}+\text{relax}}$. This term should take into account truncation of the density matrix (restricted to two levels), collisions, Van der Waals interactions, and excitation (pumping effect). Moreover, we should also include in this term coupling between atoms belonging to different velocity classes. We then focus our attention on three different types of matrix elements: first, terms linking two levels such as $\rho_{b_{m+1}a_m}(v,z,t)$ (optical coherence) and then two terms belonging to a particular state, i.e., a population such as $\rho_{a_m a_m}(v,z,t)$ and a Zeeman coherence such as $\rho_{a_m a_{m+2}}(v,z,t)$. Each of these three types will be characterized by a different relaxation constant Γ'. We obtain

$$i\hbar\left(\frac{\partial}{\partial t}+v\frac{\partial}{\partial z}+\Gamma'_a(0)\right)\rho_{a_m a_m}(v,z,t) = [\mathcal{H}_{(z,t)},\rho(v,z,t)]_{a_m a_m} + i\hbar\lambda_a, \tag{7a}$$

$$i\hbar\left(\frac{\partial}{\partial t}+v\frac{\partial}{\partial z}+\Gamma'_a(2)\right)\rho_{a_m a_{m+2}}(v,z,t) = [\mathcal{H}_{(z,t)},\rho(v,z,t)]_{a_m a_{m+2}}, \tag{7b}$$

$$i\hbar\left(\frac{\partial}{\partial t}+v\frac{\partial}{\partial z}+\Gamma'_{ab}\right)\rho_{b_{m+1}a_m}(v,z,t) = [\mathcal{H}_{(z,t)},\rho(v,z,t)]_{b_{m+1}a_m}. \tag{7c}$$

In fact, collisions and radiation effects introduce coupling between these equations. Atomic parameters (describing populations and alignment) and also optical coherences are hence modified. At low pressures, however, collision effects are small and the atomic parameters may be described in the standard $|\alpha,m\rangle$ basis[19] by the same relaxation rate; i.e., $\Gamma'(0)\sim\Gamma'(2)$. However we shall keep the notation of Eq. (7) so as to distinguish the origin of the different terms.

Two supplementary equations, analogous to (7a) and (7b), characterize the b level. λ_a and λ_b are the excitation rates per unit volume of phase space for atoms in states a and b. We suppose[1]

$$\lambda_i = \Lambda_i W_{(v)}, \quad i = a,b$$

and

$$W_{(v)} = (1/v_M\sqrt{\pi})\exp(-v^2/v_M^2)$$

is the Maxwell velocity distribution for atoms. We are looking for solutions of Eq. (7) developed in Fourier series[18]

$$\rho_{b_{m\pm1}a_m}(v,z,t) = \sum_{p=0}^{\infty}\sum_{n=-(2p+1)}^{2p+1} {}^{2p+1}_{n}\rho_{b_{m\pm1}a_m}(v)e^{-i(\omega t+nkz)}, \quad (n \text{ odd}) \tag{8a}$$

$$\rho_{a_m a_{m'}}(v,z,t) = \sum_{p=0}^{\infty}\sum_{n=-2p}^{2p} {}^{2p}_{n}\rho_{a_m a_{m'}}(v)e^{-inkz}, \quad (n \text{ even}). \tag{8b}$$

In Eq. (8b) $m' = m$ (population term) or $m' = m\pm2$ (Zeeman coherence term). The superscript $2p$ or $2p+1$ refers to the field perturbation order. Optical coherences are odd functions of the field amplitudes while the other terms (population and Zeeman coherences) are even functions. Table I shows the perturbation-iteration method used to solve (7).

In the first line of Table I there are only population terms. The second line contains only optical coherences which are proportional to the amplitude of the field. Appearing on the third line are second-order corrections to populations and also Zeeman coherence terms. The following lines contain third-order optical coherences and terms describing higher-tensorial-order J-dependent resonances[19] which will not be of interest here. Making the rotating-wave approximation, Eq. (7c) gives

$$\hbar(\omega+nkv+i\Gamma'_{ab})\,{}^{2p+1}_{n}\rho_{b_{m+1}a_m}(v) = \hbar\omega_{ab}\,{}^{2p+1}_{n}\rho_{b_{m+1}a_m}(v) - \vec{E}_1[\vec{\mu},{}^{2p}_{n+1}\rho(v)]_{b_{m+1}a_m} - \vec{E}_2[\vec{\mu},{}^{2p}_{n-1}\rho(v)]_{b_{m+1}a_m} \tag{9}$$

with

$$\Delta_n = \hbar(\omega_{ab}-\omega-nkv-i\Gamma'_{ab}). \tag{10}$$

TABLE I. Diagram representing the perturbation-iteration procedure to obtain the density matrix elements. Superscripts $2p$ or $2p+1$ refer to the field perturbation order; subscript n refers to a Fourier component. Starting with population terms in the first line one obtains optical coherence terms in the second line and so on.

								n					
p	$2p$	$2p+1$	$\cdots$	-4	-3	-2	-1	0	1	2	3	4	$\cdots$
0	0							${}^{0}_{0}\rho$					
0		1					${}^{1}_{-1}\rho$		${}^{1}_{1}\rho$				
1	2					${}^{2}_{-2}\rho$		${}^{2}_{0}\rho$		${}^{2}_{2}\rho$			
1		3			${}^{3}_{-3}\rho$		${}^{3}_{-1}\rho$		${}^{3}_{1}\rho$		${}^{3}_{3}\rho$		
2	4			${}^{4}_{-4}\rho$		${}^{4}_{-2}\rho$		${}^{4}_{0}\rho$		${}^{4}_{2}\rho$		${}^{4}_{4}\rho$	

We then find

$$\rho_{b_{m\pm1}a_m}(v,z,t) = \vec{E}_1 e^{-i(\omega t - kz)} \times \sum_p \sum_n [\vec{\mu}, {}^{2p}_{n+1}\rho(v)]_{b_{m\pm1}a_m} e^{-i(n+1)kz}/\Delta_n + \vec{E}_2 e^{-i(\omega t + kz)} \sum_p \sum_n [\vec{\mu}, {}^{2p}_{n-1}\rho(v)]_{b_{m\pm1}a_m} \times e^{-i(n-1)kz}/\Delta_n . \tag{11}$$

We have separated $\rho_{b_{m\pm1}a_m}(v,z,t)$ into two progressive parts and this will permit us to separate also $\vec{\mathcal{P}}_{(z,t)}$. This has been done so that the constitutive relation for the polarizability tensors $\underline{\alpha}_{1(z)}$ and $\underline{\alpha}_{2(z)}$ (the indices 1 and 2 stand for the propagation in positive and negative z direction) can be written as

$$\vec{\mathcal{P}}_{(z,t)} = \vec{\mathcal{P}}_{1(z,t)} + \vec{\mathcal{P}}_{2(z,t)} + \text{c.c.} = \underline{\alpha}_{1(z)} \cdot \vec{E}_1 e^{-i(\omega t - kz)} + \underline{\alpha}_{2(z)} \cdot \vec{E}_2 e^{-i(\omega t + kz)} + \text{c.c.}. \tag{12}$$

Recalling[20]

$$\vec{\mu}_{a_m b_{m\pm1}} = \mu_{a_m b_{m\pm1}}(\hat{x} \pm i\hat{y}),$$

one has

$$\vec{\mathcal{P}}_{1(z,t)} = \int_{-\infty}^{+\infty} dv \sum_m \sum_p \sum_{\substack{n=-(2p+1) \\ \text{odd}}}^{2p+1} \sum_{\epsilon=\pm1} \Delta_n^{-1} e^{-i(\omega t + nkz)} \{(\hat{x} + \epsilon i\hat{y}) \mu_{a_m b_{m+\epsilon}} \times [(\mathcal{E}_1 - i\epsilon e_1) \mu_{b_{m+\epsilon}a_m} ({}^{2p}_{n+1}\rho_{a_m a_m} - {}^{2p}_{n+1}\rho_{b_{m+\epsilon}b_{m+\epsilon}}) + (\mathcal{E}_1 + i\epsilon e_1) \times (\mu_{b_{m+\epsilon}a_{m+2\epsilon}} {}^{2p}_{n+1}\rho_{a_{m+2\epsilon}a_m} - \mu_{b_{m-\epsilon}a_m} {}^{2p}_{n+1}\rho_{b_{m+\epsilon}b_{m-\epsilon}})]\}. \tag{13}$$

$\vec{\mathcal{P}}_{1(z,t)}$ is a function of populations (first term in square brackets) and Zeeman coherences (second term in square brackets) only. This remark permits us to define the following coefficients:

$$C_p^{\pm} = \int_{-\infty}^{+\infty} dv \sum_p \sum_m \sum_{\substack{n=-(2p+1) \\ \text{odd}}}^{2p+1} \Delta_n^{-1} e^{-i(n+1)kz} \left| \mu_{a_m b_{m\pm1}} \right|^2 ({}^{2p}_{n+1}\rho_{a_m a_m}(v) - {}^{2p}_{n+1}\rho_{b_{m\pm1}b_{m\pm1}}(v)), \tag{14}$$

$$C_z^{\pm} = \int_{-\infty}^{+\infty} dv \sum_p \sum_m \sum_n \Delta_n^{-1} e^{-i(n+1)kz} [\mu_{a_m b_{m\pm1}} \mu_{b_{m\pm1}a_{m\pm2}} {}^{2p}_{n+1}\rho_{a_{m\pm2}a_m}(v) - \mu_{b_{m\mp1}a_m} \mu_{a_m b_{m\pm1}} {}^{2p}_{n+1}\rho_{b_{m\pm1}b_{m\mp1}}(v)]. \tag{15}$$

Hence, retaining $n=-1$ useful components only

$$\vec{\mathcal{P}}_{1(z,t)}=\underline{\alpha}_1\cdot(\mathcal{E}_1\hat{x}+e_1\hat{y})\exp[-i(\omega t-kz)], \tag{16a}$$

with $\underline{\alpha}_1$ now independent of z:

$$\underline{\alpha}_1=\begin{pmatrix} C_p^+ + C_p^- + C_z^+ + C_z^- & i[C_z^+ - C_z^- - C_p^+ + C_p^-] \\ i[C_p^+ - C_p^- + C_z^+ - C_z^-] & C_p^+ + C_p^- - C_z^+ - C_z^- \end{pmatrix}. \tag{16b}$$

C. Calculation of the propagation matrix

We can then deduce from $\underline{\alpha}_1$ the values of k and the corresponding eigenvectors which will furnish the desired propagation matrix. This is done in the following way. At a point z, the Maxwell propagation equation for the nonmagnetic medium, and for the complex part of the field we are interested in, takes the form

$$\operatorname{curl}\operatorname{curl}[\vec{\mathrm{E}}_1 e^{-i(\omega t-kz)}]+\frac{1}{c^2}\frac{\partial^2}{\partial t^2}[\vec{\mathrm{E}}_1 e^{-i(\omega t-kz)}] = -\mu_0\frac{\partial^2}{\partial t^2}[\underline{\alpha}_1\cdot\vec{\mathrm{E}}_1 e^{-i(\omega t-kz)}]. \tag{17}$$

The two values of k are shown to be

$$k_\pm^2=\frac{\omega^2}{c^2}[1+\mu_0 c^2(C_p^+ + C_p^-)\pm\mu_0 c^2\Delta], \tag{18}$$

where

$$\Delta=[(C_p^+ - C_p^-)^2+4C_z^+C_z^-]^{1/2}. \tag{19}$$

For a gas, $k\approx\omega/c$ and, in first approximation,

$$k_\pm=(\omega/c)[1+(1/2\epsilon_0)(C_p^+ + C_p^-)\pm(1/2\epsilon_0)\Delta]. \tag{20}$$

The propagation matrix $\underline{P}_{(dz)}$ across the slice dz is defined by

$$\vec{\mathrm{E}}_{1(z+dz)}=\underline{P}_{(dz)}\cdot\vec{\mathrm{E}}_{1(z)}, \tag{21}$$

where $\vec{\mathrm{E}}_{1(z)}$ is the complex part of the field propagating in the positive z direction. The eigenvectors corresponding to the above $k_\pm$ values define a new basis in which $\underline{P}_{(dz)}$ is diagonal. In this basis

$$\underline{P}_{(dz)}=\begin{pmatrix} e_+ & 0 \\ 0 & e_- \end{pmatrix}, \tag{22}$$

where $e_\pm=\exp(ik_\pm dz)$. The components of these eigenvectors are

$$\vec{\mathrm{V}}_\pm=\begin{pmatrix} -i(C_z^+ - C_z^- - C_p^+ + C_p^-) \\ C_z^+ + C_z^- \mp\Delta \end{pmatrix}$$

$$\text{or}\quad\begin{pmatrix} C_z^+ + C_z^- \pm\Delta \\ i(C_p^+ - C_p^- + C_z^+ - C_z^-) \end{pmatrix}, \tag{23}$$

and give the transformation matrix

$$\underline{S}=\begin{pmatrix} -i(C_p^- - C_p^+ + C_z^+ - C_z^-) & -i(C_p^- - C_p^+ + C_z^+ - C_z^-) \\ C_z^+ + C_z^- - \Delta & C_z^+ - C_z^- + \Delta \end{pmatrix}, \tag{24}$$

which provides the desired propagation matrix in the Cartesian frame,

$$\underline{P}^C_{(dz)}=\underline{S}\,\underline{P}_{(dz)}\,\underline{S}^{-1}=\tfrac{1}{2}\begin{pmatrix} e_+ + e_- + (C_z^+ + C_z^-)(e_+ - e_-)\Delta^{-1} & i(C_p^- - C_p^+ + C_z^+ - C_z^-)(e_+ - e_-)\Delta^{-1} \\ i(C_z^+ - C_z^- + C_p^+ - C_p^-)(e_+ - e_-)\Delta^{-1} & e_+ + e_- - (C_z^+ + C_z^-)(e_+ - e_-)\Delta^{-1} \end{pmatrix}. \tag{25}$$

Now let us suppose that the field amplitudes and polarizations do not change very much in the active column of the laser. The propagation matrix of the entire column, i.e., its Jones matrix $\underline{P}$, is then obtained by multiplication of the different $\underline{P}^C_{(dz)}$.[3] $\underline{P}$ is similar to expression (25) but e_+ and e_- stand now for $\exp(ik_+L)$ and $\exp(ik_-L)$, L being the active column length. Notice that the C_p^+, C_p^-, C_z^+, and C_z^- coefficients entering k are, following Eq. (16), independent of z and are also implicit functions of $|\vec{\mathrm{E}}_1|$ and $|\vec{\mathrm{E}}_2|$. We have then extended to nonlinear media the definition of the propagation matrix proposed by Jones[3] for linear crystals. This extension is only justified when the medium is such that the wave vectors do not depend on z. It corresponds to weakly saturated laser media and in this case we do not have to take into account the spatial harmonics appearing in (14) and (15) where only terms with $n=-1$ are retained. Expressions of the C_p and C_z coefficients obtained by a second-order perturbation theory are given in Appendix A.

D. Two particular cases

Having obtained the general expression for $\underline{P}$ we can now study two important particular cases. Suppose, first, that the polarization of the field is circular (either $\vec{\sigma}^+$ or $\vec{\sigma}^-$). Zeeman coherences then vanish because they can only exist via two interactions including the two polarizations $\vec{\sigma}^+$ and $\vec{\sigma}^-$. This fact can be seen from Eqs. (A10) and (A11) of Appendix A. In this case, $C_z^+=C_z^-=0$, and one obtains

$$\underline{P}_{\text{circ}}=\tfrac{1}{2}\begin{pmatrix} e_+ + e_- & -i(e_+ - e_-) \\ i(e_+ - e_-) & e_+ + e_- \end{pmatrix}, \tag{26a}$$

with

$$e_\pm=\exp(2i\pi L/\lambda)(1+C_p^\pm/\epsilon_0). \tag{26b}$$

This matrix is diagonal in the circular basis $(1, i)$ and $(1, -i)$. It has the symmetry of the saturating field. Using a probe field one observes Faraday rotation (dispersion effect) and/or circular dichroism (absorption effect). This experiment has already been done by Wieman and Hansch,[21] using a progressive circularly polarized saturating field, outside the cavity.

A second important case is the linear polarization of the field. Let $\vec{x}$ be the polarization axis. From symmetry considerations one must have $C_p^+ = C_p^- = C_p$ and $C_z^+ = C_z^- = C_z$. In deriving these equations one has to take into account that in the absence of any magnetic field only the absolute values of m have a physical meaning. The propagation matrix is

$$\underline{P}_{\text{lin}} = \begin{pmatrix} e_+ & 0 \\ 0 & e_- \end{pmatrix}, \tag{27a}$$

where

$$e_\pm = \exp(2i\pi L/\lambda)[1 + (1/\epsilon_0)(C_p \pm C_z)]. \tag{27b}$$

In this case a probe field will show birefringence and linear dichroism. It is this last effect we will describe in Sec. III.

E. General properties of the propagation matrix

In the general case, the two e.m. progressive fields do not have the same polarization. $\underline{P}$ is not diagonal in an orthonormalized basis containing one of the polarization vectors. The two wave vectors [20] will then be necessary to describe the field. In order to find the physical content of $\underline{P}$, it is convenient to use the Jones matrices $\underline{N}$.[3] They are defined as a generalization of the notion of wave numbers by the relation

$$\underline{N} = \frac{d\underline{P}}{dz}\underline{P}^{-1}.$$

The calculation gives

$$\underline{N} = \tfrac{1}{2}\begin{pmatrix} i[k_+ + k_- + (C_z^+ + C_z^-)(k_+ - k_-)\Delta^{-1}] & (C_p^+ - C_p^- - C_z^+ + C_z^-)(k_+ - k_-)\Delta^{-1} \\ -(C_p^+ - C_p^- + C_z^+ - C_z^-)(k_+ - k_-)\Delta^{-1} & i[k_+ + k_- - (C_z^+ + C_z^-)(k_+ - k_-)\Delta^{-1}] \end{pmatrix}. \tag{28}$$

The discussion of the different terms appearing in $\underline{N}$ can be done using the eight Jones matrices θ.[3] In our case it is simpler to use the Pauli matrices. $\underline{N}$ can be written as a linear combination of these matrices and the unit matrix as follows:

$$\begin{aligned} \underline{N} = {} & \tfrac{1}{2}i(k_+ + k_-)\begin{pmatrix} 1 & 0 \\ 0 & 1 \end{pmatrix} + \frac{i}{2\Delta}(C_z^+ + C_z^-)(k_+ - k_-)\begin{pmatrix} 1 & 0 \\ 0 & -1 \end{pmatrix} \\ & + \frac{i}{2\Delta}(C_p^+ - C_p^-)(k_+ - k_-)\begin{pmatrix} 0 & -i \\ i & 0 \end{pmatrix} \\ & - \frac{1}{2\Delta}(C_z^+ - C_z^-)(k_+ - k_-)\begin{pmatrix} 0 & 1 \\ 1 & 0 \end{pmatrix}. \end{aligned} \tag{29}$$

The factor of the first matrix is

$$\tfrac{1}{2}i(k_+ + k_-) = i(\omega/c)[1 + (1/2\epsilon_0)(C_p^+ + C_p^-)]. \tag{30}$$

Its real and imaginary parts give rise to the mean-amplification and phase-shifting properties of the medium. It depends only on the population of the levels.

The factor of the second matrix is

$$\frac{i}{2\Delta}(C_z^+ + C_z^-)(k_+ - k_-) = (i\omega/2\epsilon_0 c)(C_z^+ + C_z^-). \tag{31}$$

Its real and imaginary parts give rise to linear dichroism and linear-phase anisotropy (optical Kerr effect) of the active medium. Zeeman coherences are responsible for these phenomena.

The factor of the third matrix is

$$\frac{i}{2\Delta}(C_p^+ - C_p^-)(k_+ - k_-) = (i\omega/2\epsilon_0 c)[C_p^+ - C_p^-]. \tag{32}$$

Its real and imaginary parts give rise to circular dichroism and circular birefringence (optical Faraday rotation). It depends on the ellipticity of the saturating field which acts differently according to the m values of the sublevels.

The factor of the last matrix is

$$-\frac{1}{2\Delta}(C_z^+ - C_z^-)(k_+ - k_-) = (\omega/2\epsilon_0 c)(C_z^- - C_z^+). \tag{33}$$

Its real and imaginary parts give rise to linear dichroism and linear birefringence which are parallel to the bisectors of the coordinate axes.

We have now reached the following conclusion. The propagation matrix $\underline{P}$ describes the propagation of the saturating field in the active column of a weak gain laser. Its elements are functions of the polarization of the field itself. Usually, the actual polarizations correspond to those of the eigenvectors of the geometric laser cavity. It is seen now that in special cases, the active medium will also play a role in the determination of the laser eigenvectors for instance in the locking region of the Zeeman laser where the polarizations of the two counterpropagating progressive waves are not colinear in the case of a Doppler centrally tuned laser.[5]

III. EXPERIMENT

A. Analysis of the experiment

Among the different properties presented by the laser medium, we have chosen to confirm experimentally the linear anisotropy of the gain. In fact, a linearly polarized field which induces this anisotropy is what one usually finds in a laser. However, the matrix $\underline{P}_{11n}$ obtained in Sec. II applies only to the field of the laser itself. Usually, the two counterpropagating waves in the cavity have the same polarization whose direction is a principal axis of the propagation matrix. In that case the laser polarizations are independent of the induced anisotropy, and it is necessary to use a probe to test it. Figure 2 shows a diagram of laser and probe fields (paths and polarizations) in the test cell together with a definition of the coordinate axes. The probe rotates at angular frequency $2\omega_p$. The expected anisotropy signal is not exactly described by the matrix $\underline{P}_{11n}$ of the laser field but rather by the propagation matrix of the probe. We have then to determine this perturbed propagation matrix.

The origin of the coordinate axes is at the point where the interaction between the probe and the atoms begins. We shall neglect the angle between the laser and the probe light propagation axes. The probe-field vector $\vec{\mathcal{E}}_p$ can be written at $z=0$,

$$\vec{\mathcal{E}}_p = e^{-i\omega t}(e_{px}\hat{x} + e_{py}\hat{y}), \tag{34a}$$

with

$$e_{px} = e_p \cos 2\omega_p t e^{-i\phi_p}, \tag{34b}$$

$$e_{py} = e_p \sin 2\omega_p t e^{-i\phi_p}. \tag{34c}$$

The probe field appears as a small perturbation to the laser field which is also slightly modified because of the reaction of the laser. Let $\mathcal{E}_l$ be this

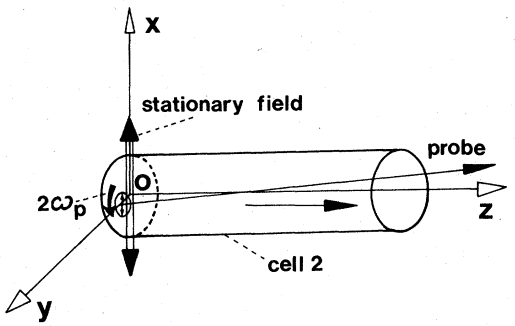

FIG. 2. Diagram of laser and probe fields (paths and polarizations) in the test cell.

new laser field. We suppose that it is polarized in the x direction and we designate by ϕ_p the phase of the probe relative to that of the laser field at $z=0$. The total field at a point z in the test tube is given by Eqs. (1) and (2) with

$$\begin{aligned} &\mathcal{E}_1 = \mathcal{E}_l + e_p \cos 2\omega_p t\, e^{-i\phi_p}, \quad \mathcal{E}_2 = \mathcal{E}_l \\ &e_1 = e_p \sin 2\omega_p t\, e^{-i\phi_p}, \quad e_2 = 0. \end{aligned} \tag{35}$$

The probe field induces a change of the polarization

$$d\vec{\mathcal{P}}_{1(z)} = \underline{\alpha}_1 \cdot \vec{\mathcal{E}}_p e^{ikz} + d\underline{\alpha}_1 \cdot \vec{\mathcal{E}}_1 e^{-i(\omega t - kz)}. \tag{36}$$

$\underline{\alpha}_1$ is the polarizability containing $\mathcal{E}_l$, and $d\underline{\alpha}_1$ stands for the variation of $\underline{\alpha}_1$ due to the probe. The Maxwell Eq. (17) applied to the total field (35) is written

$$\begin{aligned} \left(k^2 - \frac{\omega^2}{c^2}\right)(\vec{\mathcal{E}}_l e^{-i(\omega t - kz)} + \vec{\mathcal{E}}_p e^{ikz}) \\ = \mu_0 \omega^2 (\underline{\alpha}_1 + d\underline{\alpha}_1)(\vec{\mathcal{E}}_l e^{-i(\omega t - kz)} + \vec{\mathcal{E}}_p e^{ikz}), \end{aligned} \tag{37}$$

and leads to the eigenvalue problem,

$$\begin{vmatrix} \alpha_{11} + d\alpha_{11} - \left(k^2 - \frac{\omega^2}{c^2}\right)/\mu_0\omega^2 & d\alpha_{12} \\ d\alpha_{21} & \alpha_{22} + d\alpha_{22} - \left(k^2 - \frac{\omega^2}{c^2}\right)/\mu_0\omega^2 \end{vmatrix} = 0. \tag{38}$$

Now we shall use the coefficients C_p^+, C_p^-, C_z^+, and C_z^- calculated by a second-order perturbation theory in Appendix A and we obtain

$$\alpha_{11} = -\frac{2N_0 S}{\hbar k v_M} Z_{(i)} + \frac{2N_0}{i\hbar}\mathcal{E}_l^2 (I_1 + I_2)\left(\frac{S_1+S_3}{\Gamma_a'(0)} + \frac{S_1+S_2}{\Gamma_b'(0)} + \frac{S_2}{\Gamma_a'(2)} + \frac{S_3}{\Gamma_b'(2)}\right), \tag{39a}$$

α_{22}: identical expression but with a minus sign before $\Gamma_a'(2)$ and $\Gamma_b'(2)$. (39b)

$$d\alpha_{11} = \frac{2N_0 \mathcal{E}_l I_1}{i\hbar}(e_{px} + e_{px}^*)\left(\frac{S_1+S_3}{\Gamma_a'(0)} + \frac{S_1+S_2}{\Gamma_b'(0)} + \frac{S_2}{\Gamma_a'(2)} + \frac{S_3}{\Gamma_b'(2)}\right), \tag{39c}$$

$d\alpha_{22}$: identical expression but with a minus sign before $\Gamma_a'(2)$ and $\Gamma_b'(2)$. (39d)

$$d\alpha_{12} = 2i\frac{N_0 \mathcal{E}_1 I_1}{\hbar}\left[(e_{py} - e_{py}^*)\left(\frac{S_1 - S_3}{\Gamma_a'(0)} + \frac{S_1 - S_2}{\Gamma_b'(0)}\right) - (e_{py} + e_{py}^*)\left(\frac{S_2}{\Gamma_a'(2)} + \frac{S_3}{\Gamma_b'(2)}\right)\right], \tag{39e}$$

$$d\alpha_{21} = -2i\frac{N_0 \mathcal{E}_1 I_1}{\hbar}\left[(e_{py} - e_{py}^*)\left(\frac{S_1 - S_3}{\Gamma_a'(0)} + \frac{S_1 - S_2}{\Gamma_b'(0)}\right) + (e_{py} + e_{py}^*)\left(\frac{S_2}{\Gamma_a'(2)} + \frac{S_3}{\Gamma_b'(2)}\right)\right]. \tag{39f}$$

Equation (38) gives the following eigenvalues:

$$\frac{1}{\mu_0\omega^2}\left(k^2 - \frac{\omega^2}{c^2}\right) = -\frac{2N_0 S}{\hbar k v_M} Z(\xi) + \frac{2N_0}{i\hbar}\mathcal{E}_1^2(I_1 + I_2)\left(\frac{S_1 + S_3}{\Gamma_a'(0)} + \frac{S_1 + S_2}{\Gamma_b'(0)}\right)$$
$$+ \frac{4N_0}{i\hbar} I_1 \mathcal{E}_1 e_p \cos 2\omega_p t \cos\phi_p \left(\frac{S_1 + S_3}{\Gamma_a'(0)} + \frac{S_1 + S_2}{\Gamma_b'(0)}\right) \pm \tfrac{1}{2}\{[\alpha_{11} - \alpha_{22} + b_x(\phi_p)]^2 - b_y(\phi_p)\}^{1/2}, \tag{40}$$

where

$$b_x(\phi_p) = \frac{8N_0}{i\hbar} I_1 \mathcal{E}_1 e_p \cos 2\omega_p t \cos\phi_p \left(\frac{S_2}{\Gamma_a'(2)} + \frac{S_3}{\Gamma_b'(2)}\right), \tag{41a}$$

$$b_y(\phi_p) = \frac{64N_0^2}{\hbar^2} I_1^2 \mathcal{E}_1^2 e_p^2 \sin^2 2\omega_p t\left[\sin^2\phi_p \left(\frac{S_1 - S_3}{\Gamma_a'(0)} + \frac{S_1 - S_2}{\Gamma_b'(0)}\right)^2 - \cos^2\phi_p \left(\frac{S_2}{\Gamma_a'(2)} + \frac{S_3}{\Gamma_b'(2)}\right)^2\right]. \tag{41b}$$

Taking into account that $e_p \ll \mathcal{E}_1$ we shall neglect coupling terms ($e_p\mathcal{E}_1$ terms) versus main saturation terms ($\mathcal{E}_1^2$ terms). In this approximation the corresponding eigenvectors given by (23) are also found to be along $\hat{x}$ and $\hat{y}$. Calling then k_x and k_y the two above k eigenvalues, the output probe field may be written

$$\vec{e}_{px(L)} = e_{px}\exp(ik_x L)\hat{x}, \tag{42}$$

$$\vec{e}_{py(L)} = e_{py}\exp(ik_y L)\hat{y}. \tag{43}$$

Moreover the probe field is also amplified in the volume of the cell not filled by the laser beam. $\kappa_{(\nu)}$ is the isotropic factor describing this amplification. The output signal will then have the intensity

$$|\vec{e}_{px(L)}|^2 + |\vec{e}_{py(L)}|^2 = |\kappa_{(\nu)}|^2 e_p^2[\cos^2 2\omega_p t\, e^{2k_x^i L} + \sin^2 2\omega_p t e^{2k_y^i L}], \tag{44}$$

where k^i is the imaginary part of k(Imk). Assuming that k^i is weak, one can make the first-order expansion

$$e^{2k^i L} \approx 1 + 2k^i L. \tag{45}$$

The phase-detection output will give only the $4\omega_p$ modulated signal

$$\Delta I = |\kappa_{(\nu)}|^2 e_p^2 (k_x^i - k_y^i) L, \tag{46}$$

with

$$k_x^i - k_y^i = -\frac{\omega}{2\epsilon_0 c}\,\mathrm{Im}\,[(\alpha_{11} - \alpha_{22} + b_x(\phi_p))^2 - b_y(\phi_p)]^{1/2}. \tag{47}$$

The difference $\alpha_{11} - \alpha_{22}$ represents the limit of the gas anisotropy when the intensity of the probe vanishes:

$$\alpha_{11} - \alpha_{22} = \frac{4N_0}{i\hbar}\mathcal{E}_1^2(I_1 + I_2)\left(\frac{S_2}{\Gamma_a'(2)} + \frac{S_3}{\Gamma_b'(2)}\right). \tag{48}$$

We have already seen that it is only due to Zeeman coherences. As described later we have modulated the phase ϕ_p of the probe in order to avoid spurious interference effects between laser and probe beams. Note that this modulation also simplifies the above expressions (41a) and (41b) of the small $b_x(\phi_p)$ and $b_y(\phi_p)$ terms. The expression for the signal obtainable by the apparatus of Fig. 4 Scheme 2 described in Sec. III(B) is then in first approximation

$$\frac{\Delta I}{\kappa^2_{(\nu)} e_p^2 \mathcal{E}_1^2} = \frac{2\omega L N_0}{\epsilon_0 c\hbar}\left(\frac{S_2}{\Gamma_a'(2)} + \frac{S_3}{\Gamma_b'(2)}\right)\mathrm{Re}(I_1 + I_2). \tag{49}$$

The experiment has been done using $3s_2(J_b = 1)$ and $3p_4(J_a = 2)$ levels of Ne^{20}. In this case $S_2/S_3 = 21$ and we can neglect the contributions of the $3s_2$ level.[22] In these conditions, the signal (49) is proportional to $\mathrm{Re}(I_1 + I_2)$. Figure 3 shows this function for various values of $y = \Gamma_{ab}'/kv_M$. We notice that function I_2 is narrower than function I_1 according to their definitions (A18) and (A17), given in the Appendix. Physically, I_1 describes the saturation caused by the progressive waves while I_2 describes saturation due to two counterpropagating waves interacting with the same atom velocity group.

We should notice that in our experiment the contribution due to linear dichroism is separated from that due to linear birefringence. This is in opposition to Wieman and Hänsch's experiment in which circular dichroism and birefringence are intermingled.[21]

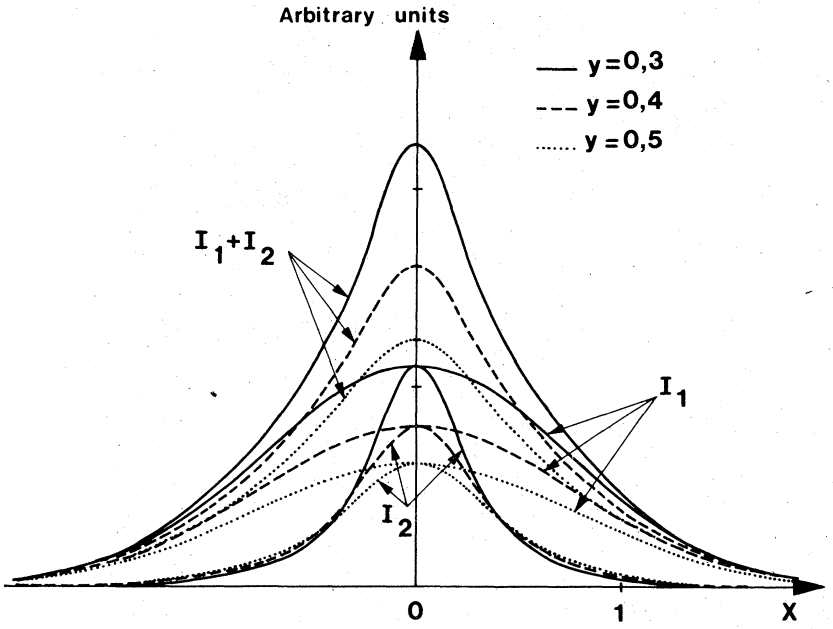

FIG. 3. Theoretical curves showing the real parts of the functions I_1, I_2 and I_1+I_2 [see Eqs. (A17) and (A18)] versus $(\omega-\omega_{ab})/kv_M$ for three y values ($y=\Gamma'_{ab}/kv_M$). Full line, $y=0.3$. Dashed line, $y=0.4$. Dotted line, $y=0.5$.

B. Experimental apparatus

In order to have a matching of the probe and laser frequencies it would be possible to use a part of the output laser light. Rotating the probe polarization would then permit us to detect the gain anisotropy via a phase detection. However, this method does not permit one to give the zero signal we would expect if the saturating field was absent because switching off the laser also switches off the probe. This is why we have set up the experiment as pictured in Fig. 4. The active column is made of two separate tubes filled with the same He-Ne gas. The first tube has a gain sufficient to maintain the laser operation even when the second one is switched off. The probe goes through this test tube and one finds the zero signal. We then observe the anisotropy signal.

The monomode laser works on the 3.39 μm line of Ne^{20} ($3s_2-3p_4$ levels). The cavity is 38 cm long ($c/2L=394$ MHz) and contains the following between its end mirrors M_1 and M_2 (see Fig. 4):

(1) A Brewster windows-ended tube 14 cm long and 1.5 mm inside diameter. It maintains oscillation and, thanks to the Brewster windows, a fixed linear polarization of the field in the first part of the laser.

(2) An antireflection coated half-wave plate $\frac{1}{2}\lambda_i$ which can be used to change, in a controlled manner, the orientation of the linear polarization in the second part of the cavity.

(3) A test tube 12 cm long which constitutes this second part. This tube is closed by two windows which are almost perpendicular to the laser axis and do not modify appreciably the linear polarization of the laser field. A pipe connection between the two tubes assures us that the composition and the pressure of the gas in them are the same. The diameter of this test cell was chosen to be

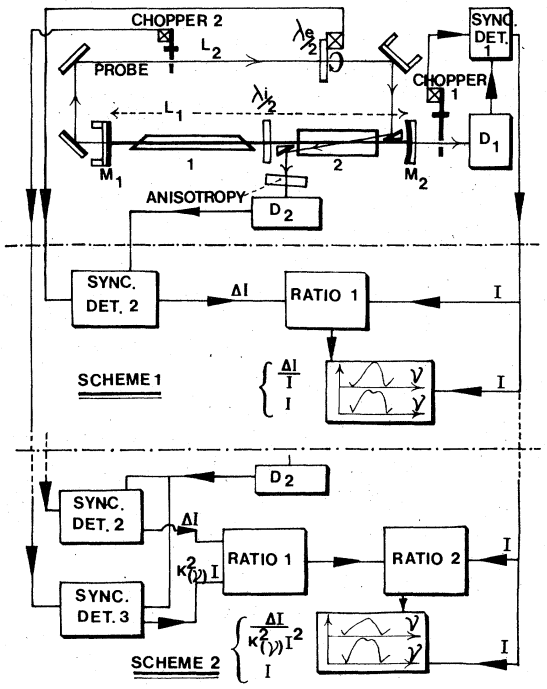

FIG. 4. Diagram of the experimental setup. Tube 1 maintains the oscillation. Tube 2 is the test cell. The $\frac{1}{2}\lambda_e$ plate, turning at ω_p, rotates the polarization of the probe at $2\omega_p$. The polarization of the laser field in the test cell can be varied by the $\frac{1}{2}\lambda_i$ plate.

4.5 mm to allow the propagation of the probe beam along an axis making a slight angle (≈0.5°) with the laser beam. We put two diaphragms with two holes at the ends of the cell to achieve separation for the beams outside, and maximum overlapping inside. The overlapping volume is approximately equal to half the volume of the cell. Preliminary adjustments of these diaphragms were made with an auxiliary 6328 Å laser. Outside the cavity we put the following:

(i) A half-wave plate $\frac{1}{2}\lambda_e$ which receives the fixed linear polarization of the output laser field emerging from the end mirror M_1. This plate is rotated at a constant rate of 3 Hz and this causes the plane of polarization of the emerging beam (the probe) to rotate at twice this frequency.

(ii) Attenuators which can weaken the intensity of the probe.

(iii) Several mirrors to achieve the light path L_2 indicated in Fig. 4. One of these mirrors is mounted on a P.Z.T. supplied by a ramp generator. This device permits us to get rid of interference effects between probe and laser beams by a rapid modulation of their relative phase angle ϕ_p.

Using this apparatus we obtain:

(a) Laser light intensity I vs frequency. A slow frequency tuning was obtained with the mirror M_1 mounted also on a P.Z.T.

(b) The variation of the gain anisotropy ΔI (intensity of the probe signal modulated at $4\omega_p$) vs frequency. ΔI is detected by a phase-sensitive amplifier whose reference frequency is 4 times the rotation frequency of the $\frac{1}{2}\lambda_e$ plate. The two curves I and ΔI can be simultaneously recorded and we have also recorded the normalized gain anisotropy $\Delta I/I$ using a ratiometer (Fig. 4, Scheme 1).

(c) The curve proportional to the calculated signal. The parameter $\kappa_{(\nu)}$ takes into account the isotropic gain in the nonsaturated part of the gas tested by the probe. $\kappa_{(\nu)}$ is obtained by chopping the probe and measuring its output intensity proportional to $\kappa^2_{(\nu)}I$. Using a first ratiometer as indicated in Fig. 4 (Scheme 2) we obtain $\Delta I/\kappa^2_{(\nu)}I$. Then a second ratiometer normalizes this quantity according to the intensity of the saturating field. This last ratio characterizes the anisotropy as a function of the frequency in the third perturbation order and is given by Eq. (49).

C. Experimental results

First we have to obtain the null signal when the test tube is switched off. As has been said before, the end windows of the cell are not exactly perpendicular to the axis of the laser. The Fresnel transmission coefficients for the two polarization amplitudes e_{px} and e_{py} are not the same and this gives rise to an undesired anisotropic signal. These windows act like a partial polarizer and it is easy to compensate their effect using another partial polarizer. For this purpose we have simply used a laser window properly oriented in front of the detector. After that the test tube is switched on and we obtain a $4\omega_p$ signal as shown in Figs. 5 and 6. In Fig. 5, the lower curve (Fig. 5c) shows a reference voltage obtained via the photodiode in the chopper system coupled with the rotating $\frac{1}{2}\lambda_e$ plate. Each time the laser and probe polarizations are parallel, the probe gain is minimal. This situation happens at angles separated by 90° of the $\frac{1}{2}\lambda_e$ plate. If we rotate the $\frac{1}{2}\lambda_i$ plate by an angle 45°, the laser polarization is changed by 90° and the respective positions of minima and maxima are interchanged as shown in Fig. 5b. In this case instead of Eq. (35) one has, for the field,

$$\mathcal{E}_1 = e_p \cos 2\omega_p t\, e^{-i\phi_p}, \quad \mathcal{E}_2 = 0,$$
$$e_1 = \mathcal{E}_1 + e_p \sin 2\omega_p t\, e^{-i\phi_p}, \quad e_2 = \mathcal{E}_1. \tag{35'}$$

The equations indicate the above polarization change. This change results in replacing $\vec{e}_{px}$ by $\vec{e}_{py}$ and vice versa in the preceding equations, which simply leads to an opposite sign in the detected signal (49). The experimental results shown in Figs. 5 and 6 agree with this prediction. The order of magnitude of $\Delta I/e_p^2$ is 4% when the discharge current is 12 mA. This is comparable with loss anisotropies introduced by a SiO_2 plate and usually defined[2] by the ratio $(r_x - r_y)/(r_x + r_y)$. This ratio is of the order of 11% for a Brewster window and corresponds here to 2%. Simultaneous recordings of I and $\Delta I/\kappa^2_{(\nu)}I^2$ are shown in Fig. 6. The total pressure was 1.2 Torr ($Ne^{20}/He^3 \simeq \frac{1}{7}$). We

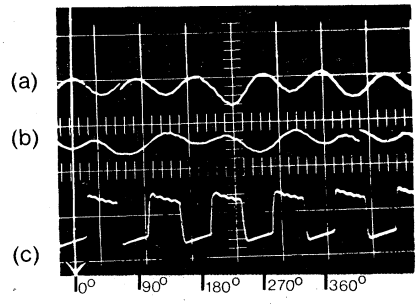

FIG. 5. Observation of the optical anisotropy induced by the saturating field. (a) Portion of the probe modulated at $4\omega_p$ (test tube switched on). (b) Portion of probe output modulated at $4\omega_p$ with the polarization of the laser field rotated by 90° as compared to preceding curve. This rotation has been obtained from a rotation by 45° of the $\frac{1}{2}\lambda_i$ plate. (c) Signal in phase with the rotation of the $\frac{1}{2}\lambda_e$ plate (one cycle corresponds to a rotation of 90°).

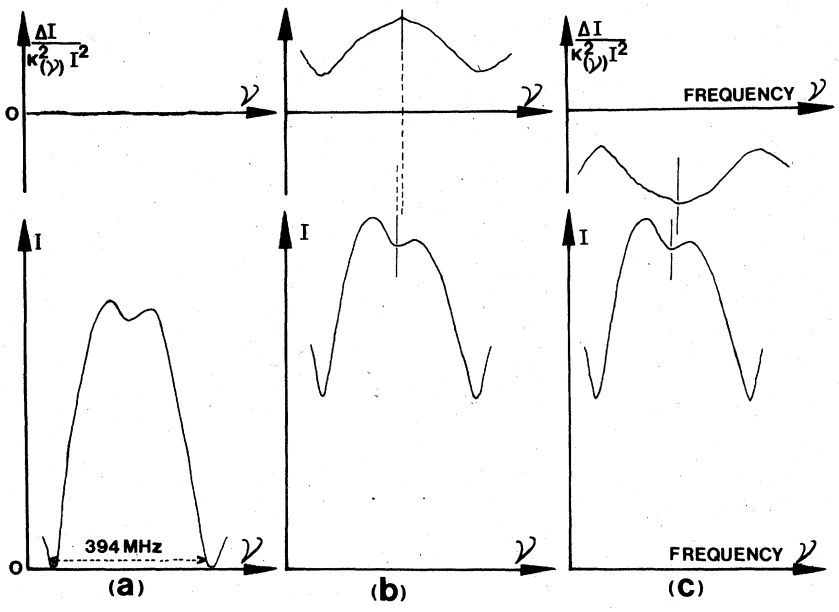

FIG. 6. Simultaneous recordings of output laser light I (lower curves) (mode spacing $= c/2L_1 = 394$ MHz; output power about 15 μW) and normalized ratios $\Delta I/\kappa^2_{(\nu)} I^2$ (upper curves) vs frequency for three cases: (a) Test tube switched off. Null signal observed. (b) Test tube switched on, polarization of the laser field in the incidence plane of the Brewster windows. (c) The same with the polarization of the laser rotated by 90°.

note an asymmetry of the Lamb dip which has been already seen by Bennett[23] at 3.39 μm. We note also that the center of the anisotropy curve does not correspond to the center of the Doppler profile.[24] These two effects are outside the scope of this paper and will be the subjects of future studies. Simultaneous recordings of $\Delta I/I$ and I as given by Scheme 1 of our experimental arrangement (Fig. 4) are shown in Fig. 7(a). The contribution of the I_2 Lorentzian integral to the shape of the $\Delta I/I$ signal is to be noticed near line center. Taking into account expected phase-changing collision effects,[25] which have been ignored in our calculations, only 10 to 20% of the Lorentzian signal is to be considered. A fit of theoretical and experimental results is given on Fig. 7(b) where dots represent calculated values of $\mathrm{Re}(I_1 + 0.2I_2)$ for $y = 0.4$. At line wings there are perturbations due to undesired two-mode operation; theoretical points for $1 \leq |x| \leq 1.4$ are then translated on the dashed line.

IV. CONCLUSION

In the course of this work we have first defined the propagation matrix for the saturating optical field in the "atoms + field" medium of a weakly saturated gas laser. In fact, this matrix corresponds to the type Jones qualified in 1942[3] as "nonphysically realizable" because it corresponded to an amplifying medium. We have shown that $\underline{P}$ depends on the properties of the atoms (velocity

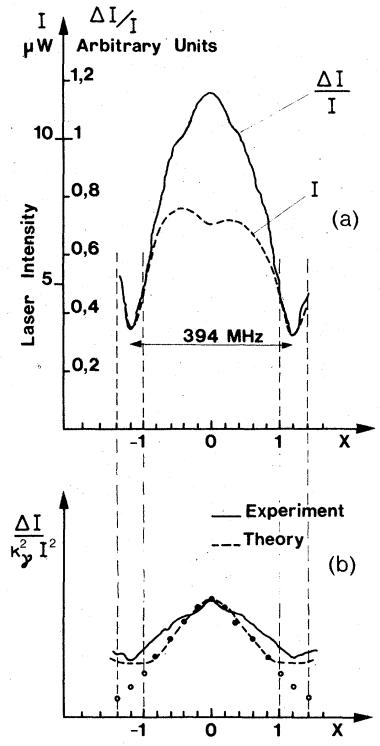

FIG. 7. Experimental and theoretical data. (a) Simultaneous recordings of $\Delta I/I$ and I. (b) The anisotropy signal. Dots represent calculated values of $\mathrm{Re}(I_1 + 0.2I_2)$ for $y = 0.4$ and Doppler width 330 MHz. The dashed line takes into account the contribution of two-mode operation for $1 \leq |x| \leq 1.4$.

distribution, energies, lifetime, and angular momentum of the levels ...) and also on the parameters of the field (amplitude, frequency, polarization...). It corresponds to the matrix of a medium made up of an "atoms + field" system. In this medium various anisotropies occur and we have chosen to verify experimentally one of them: the linear gain anisotropy which appears when the laser field is linearly polarized and which results from Zeeman coherences between sublevels. The described experiment is new and shows the predicted effect. Such a $\underline{P}$ matrix will be used in the application of the resonance condition for the research of the eigenvectors each time one of the two following conditions are satisfied: (i) the anisotropies of the cavities and those of the active medium are of the same order of magnitude; and (ii) the two counter-propagating waves have different polarizations. The use of a $\underline{P}$ matrix can also be justified in problems of saturation spectroscopy. Our experimental result shows a different displacement of the nonlinear anisotropy signal versus the Doppler profile. This leads to effects on the output light of the laser and may be related to the asymmetry of the Lamb dip. Further studies are in progress to show its dependence on polarization and frequency in particular cases.

ACKNOWLEDGMENTS

We are happy to thank Professor M. Trümper for his active interest during the preparation of the final manuscript, and also J. Guilloux, J. L. Steinhardt, and H. Gehanno for construction of parts of the experimental apparatus.

APPENDIX A

In this appendix we calculate in a second-order approximation the coefficients C_p^+, C_p^-, C_z^+, and C_z^- defined by Eqs. (14) and (15). The calculation is similar to that usually found in the literature.

We suppose that Zeeman coherences are initially zero and, in first order, we write for the populations

$$ {}^0_0\rho_{a_m a_m} = [\Lambda_a/\Gamma'_a(0)]W_{(v)}\,, \quad {}^0_0\rho_{b_m b_m} = [\Lambda_b/\Gamma'_b(0)]W_{(v)}\,. \tag{A1}$$

$\Lambda_a(\Lambda_b)$ is the number of atoms in the excited state a (b) per unit volume and time. $\Gamma'_a(0)$ $[\Gamma'_b(0)]$ is the a $[b]$ level population relaxation coefficient. We suppose it is real and independent of the velocity v and of the magnetic quantum number m. $W_{(v)}$ is the normalized Maxwell velocity distribution function. If we define

$$ {}^0_0\rho_{b_m b_m}(v) - {}^0_0\rho_{a_m a_m}(v) = \left(\frac{\Lambda_b}{\Gamma'_b(0)} - \frac{\Lambda_a}{\Gamma'_a(0)}\right) W_{(v)} = N_0 W_{(v)}\,, \tag{A2}$$

we obtain, using Eq. (9), optical coherences in first order

$$ \begin{aligned} {}^1_1\rho_{b_{m+1}a_m}(v) &= -\frac{N_0 W_{(v)}}{\Delta_1}(\mathcal{E}_2 \mp i e_2)\mu_{b_{m+1}a_m}\,, \\ {}^1_{-1}\rho_{b_{m+1}a_m}(v) &= -\frac{N_0 W_{(v)}}{\Delta_{-1}}(\mathcal{E}_1 \mp i e_1)\mu_{b_{m+1}a_m}\,. \end{aligned} \tag{A3}$$

In second order we then obtain populations which are the diagonal elements of the density matrix and we also obtain Zeeman coherences linking two sublevels with $\Delta m = 2$. Using (7a) and (8b) with $m = m'$ we can write

$$ \begin{aligned} i\hbar\Gamma'_a(0)\,{}^2_0\rho_{a_m a_m}(v) &= -\vec{E}(\vec{\mu}, \rho)_{a_m a_m} \\ &= -\vec{E}(\vec{\mu}_{a_m b_{m+1}}\rho_{b_{m+1}a_m} + \vec{\mu}_{a_m b_{m-1}}\rho_{b_{m-1}a_m} - \rho_{a_m b_{m+1}}\vec{\mu}_{b_{m+1}a_m} - \rho_{a_m b_{m-1}}\vec{\mu}_{b_{m-1}a_m})\,. \end{aligned} \tag{A4}$$

Defining

$$ \begin{aligned} s_1^+ &= \mathcal{E}_1 + i e_1\,, \quad s_1^- = \mathcal{E}_1 - i e_1\,, \\ s_2^+ &= \mathcal{E}_2 + i e_2\,, \quad s_2^- = \mathcal{E}_2 - i e_2\,, \end{aligned} \tag{A5}$$

one obtains

$$ \begin{aligned} {}^2_0\rho_{a_m a_m}(v) = \frac{N_0 W_{(v)}}{i\hbar\Gamma'_a(0)}\Bigg[&\left(\frac{1}{\Delta_1} - \frac{1}{\Delta_1^*}\right)\left(|\mu_{a_m b_{m+1}}|^2 |s_2^-|^2 + |\mu_{a_m b_{m-1}}|^2 |s_2^+|^2\right) \\ &+ \left(\frac{1}{\Delta_{-1}} - \frac{1}{\Delta_{-1}^*}\right)\left(|\mu_{a_m b_{m+1}}|^2 |s_1^-|^2 + |\mu_{a_m b_{m-1}}|^2 |s_1^+|^2\right)\Bigg]. \end{aligned} \tag{A6}$$

Following the same procedure one obtains also

$$ {}^2_0\rho_{b_m b_m}(v)=\frac{N_0 W_{(v)}}{i\hbar\Gamma'_b(0)}\left[\left(\frac{1}{\Delta_1^*}-\frac{1}{\Delta_1}\right)\left(|\mu_{b_m a_{m+1}}|^2|s_2^+|^2+|\mu_{b_m a_{m-1}}|^2|s_2^-|^2\right)\right. $$

$$ \left.+\left(\frac{1}{\Delta_{-1}^*}-\frac{1}{\Delta_{-1}}\right)\left(|\mu_{b_m a_{m+1}}|^2|s_1^+|^2+|\mu_{b_m a_{m-1}}|^2|s_1^-|^2\right)\right]. \tag{A7} $$

Calculation of the second-order Zeeman coherences is performed using the same method

$$ i\hbar\Gamma'_a(2)\,{}^2_0\rho_{a_m a_{m+2}}(v)=-\vec{E}\left[\vec{\mu},\sum_{n=\pm1}{}^1_n\rho(v)\right]_{a_m a_{m+2}} \tag{A8} $$

$$ =-\vec{E}\left(\vec{\mu}_{a_m b_{m+1}}\sum_{n=\pm1}{}^1_n\rho_{b_{m+1}a_{m+2}}-\vec{\mu}_{b_{m+1}a_{m+2}}\sum_{n=\pm1}{}^1_n\rho_{a_m b_{m+1}}+\vec{\mu}_{a_m b_{m-1}}\sum_{n=\pm1}{}^1_n\rho_{b_{m-1}a_{m+2}}\right. $$

$$ \left.-\vec{\mu}_{b_{m+3}a_{m+2}}\sum_{n=\pm1}{}^1_n\rho_{a_m b_{m+3}}\right). \tag{A9} $$

One should notice the cancellation of the two last terms because optical coherences with $\Delta m=3$ do not exist in this perturbation order. One then deduces

$$ {}^2_0\rho_{a_m a_{m+2}}(v)=\frac{N_0 W_{(v)}}{i\hbar\Gamma'_a(2)}\mu_{a_m b_{m+1}}\mu_{b_{m+1}a_{m+2}} $$

$$ \times\left[s_1^+ s_1^{-*}\left(\frac{1}{\Delta_{-1}}-\frac{1}{\Delta_{-1}^*}\right)+s_2^+ s_2^{-*}\left(\frac{1}{\Delta_1}-\frac{1}{\Delta_1^*}\right)\right]. \tag{A10} $$

An expression for $\rho_{a_m a_{m-2}}$ can be deduced from (A10) by replacing $m\to m-2$ and taking the complex conjugate. One also obtains

$$ {}^2_0\rho_{b_m b_{m+2}}(v)=\frac{N_0 W_{(v)}}{i\hbar\Gamma'_b(2)}\mu_{b_m a_{m+1}}\mu_{a_{m+1}b_{m+2}} $$

$$ \times\left[s_2^+ s_2^{-*}\left(\frac{1}{\Delta_1^*}-\frac{1}{\Delta_1}\right)+s_1^+ s_1^{-*}\left(\frac{1}{\Delta_{-1}^*}-\frac{1}{\Delta_{-1}}\right)\right]. \tag{A11} $$

We shall use these expressions to write the C_p^+, C_p^-, C_z^+ and C_z^- coefficients using Eqs. (14) and (15). In zero order, the C_p^+ and C_p^- coefficients are

$$ {}^0C_p^{\pm}=\int_{-\infty}^{+\infty}dv\sum_m\frac{-1}{\Delta_{-1}}|\mu_{a_m b_{m\pm1}}|^2 N_0 W_{(v)} $$

$$ =\frac{-N_0 S}{\hbar k v_M}Z_{(\xi)}, \tag{A12} $$

where we have to take $k=\omega/c$. $Z_{(\xi)}$ is the plasma dispersion function.[26] $\xi=x+iy$ where

$$ x=(\omega-\omega_{ab})/kv_M \quad\text{and}\quad y=\Gamma'_{ab}/kv_M. \tag{A13} $$

Moreover, we took

$$ S=\sum_m|\mu_{a_m b_{m\pm1}}|^2. \tag{A14} $$

In second order, one then obtains

$$ {}^2C_p^+=\frac{N_0}{i\hbar}\left[(I_1|s_1^+|^2+I_2|s_2^+|^2)\left(\frac{S_2}{\Gamma'_b(0)}+\frac{S_3}{\Gamma'_a(0)}\right)\right. $$

$$ \left.+(I_1|s_1^-|^2+I_2|s_2^-|^2)\left(\frac{S_1}{\Gamma'_a(0)}+\frac{S_1}{\Gamma'_b(0)}\right)\right], \tag{A15} $$

$$ {}^2C_p^-=\frac{N_0}{i\hbar}\left[(I_1|s_1^+|^2+I_2|s_2^+|^2)\left(\frac{S_1}{\Gamma'_a(0)}+\frac{S_1}{\Gamma'_b(0)}\right)\right. $$

$$ \left.+(I_1|s_1^-|^2+I_2|s_2^-|^2)\left(\frac{S_2}{\Gamma'_b(0)}+\frac{S_3}{\Gamma'_a(0)}\right)\right]. \tag{A16} $$

If we define

$$ I_1=\int_{-\infty}^{+\infty}\frac{W_{(v)}}{\Delta_{-1}}\left(\frac{1}{\Delta_{-1}}-\frac{1}{\Delta_{-1}^*}\right)dv $$

$$ =\frac{1}{(\hbar k v_M)^2}\left(Z'_{(\xi)}-\frac{1}{y}Z^i_{(\xi)}\right), \tag{A17} $$

$$ I_2=\int_{-\infty}^{+\infty}\frac{W_{(v)}}{\Delta_{-1}}\left(\frac{1}{\Delta_1}-\frac{1}{\Delta_1^*}\right)dv $$

$$ =\frac{1}{(\hbar k v_M)^2}\left(\frac{1}{x}Z'_{(\xi)}-\frac{1}{\xi}Z_{(\xi)}\right), \tag{A18} $$

in the Doppler limit, the imaginary part of ξ vanishes and I_2 describes a Lorentzian. $Z'_{(\xi)}$ and $Z^i_{(\xi)}$ stand respectively for the real and imaginary part of the plasma dispersion function. The sums over m appearing in Eqs. (A15) and (A16) are

$$ S_1=\sum_m|\mu_{a_m b_{m+1}}|^4, \tag{A19} $$

$$ S_2=\sum_m|\mu_{a_m b_{m+1}}|^2|\mu_{b_{m+1}a_{m+2}}|^2, \tag{A20} $$

$$S_3 = \sum_m |\mu_{a_m b_{m+1}}|^2 |\mu_{a_m b_{m-1}}|^2 . \quad \text{(A21)}$$

These sums,[27] as well as the integrals I_1 and I_2,[1] appear frequently in the literature. Expressions for the coefficients depending on Zeeman coherences are

$$^2C_z^+ = \frac{N_0}{i\hbar}\left(\frac{S_2}{\Gamma_a'(2)} + \frac{S_3}{\Gamma_b'(2)}\right)\left(I_1 s_1^- s_1^{+*} + I_2 s_2^- s_2^{+*}\right) , \quad \text{(A22)}$$

$$^2C_z^- = \frac{N_0}{i\hbar}\left(\frac{S_2}{\Gamma_a'(2)} + \frac{S_3}{\Gamma_b'(2)}\right)\left(I_1 s_1^+ s_1^{-*} + I_2 s_2^+ s_2^{-*}\right) . \quad \text{(A23)}$$

---

*On leave of absence from U.E.R. "S.P.M.", Université de Rennes, BP 25A, Rennes, 35031, France.

[1]W. E. Lamb Jr., Phys. Rev. 134, A1429 (1964); M. Sargent III, M. O. Scully, and W. E. Lamb Jr., *Laser Physics* (Addison Wesley, Reading, Mass., 1974).
[2]A. Le Floch and R. Le Naour, Phys. Rev. A 4, 290 (1971).
[3]R. C. Jones, J. Opt. Soc. Am. 38, 671 (1948) and previous papers of the series.
[4]A. Le Floch and G. Stephan, Phys. Rev. A 6, 845 (1972).
[5]A. Le Floch and G. Stephan, C. R. Acad. Sci. 274, 491 (1972).
[6]A. Le Floch and G. Stephan, C. R. Acad. Sci. 277b, 265 (1973).
[7]A. Le Floch and G. Stephan, Rev. Phys. Appl. 10, 1 (1975).
[8]W. Happer, Prog. Quantum Electron. 1, 53 (1970).
[9]W. M. Doyle and M. B. White, Phys. Rev. 147, 359 (1966).
[10]H. De Lang and G. Bouwhuis, Phys. Lett. 19, 482 (1965); H. De Lang, Ph.D. thesis (University of Utrech, 1966) (unpublished).
[11]W. Van Haeringen, Phys. Rev. 158, 256 (1967).
[12]A. Dienes, IEEE J. Quantum Electron. 5, 162 (1969).
[13]Im. Thek-de, S. G. Rautian, E. G. Saprykin, G. I. Smirnov, and A. M. Shalagin, Zh. Eksp. Teor. Fiz. 62, 1661 (1972) [Sov. Phys. JETP 35, 865 (1972)].
[14]Yu. A. Vdovin, V. M. Ermachenko, A. I. Popov, and E. D. Protsenko, Zh. Eksp. Teor. Fiz. Pis. Red. 15, 401 (1972) [Sov. Phys. JETP Lett. 15, 282 (1972)].
[15]C. V. Shank and S. E. Schwarz, IEEE J. Quantum Electron. 4, 1017 (1966).
[16](a) H. Greenstein, Phys. Rev. 178, 585 (1969); (b) W. G. Guion and J. P. Craig, Proc. IEEE 56, 1624 (1968); Di Chen *et al.*, IEEE J Quantum Electron. 2, 461 (1966); 6, 259 (1970).
[17]M. Sargent III, W. E. Lamb Jr., and R. L. Fork, Phys. Rev. 164, 436 (1967); 164, 450 (1967).
[18]B. J. Feldman and M. S. Feld, Phys. Rev. A 1, 1375 (1970); S. Haroche and F. Hartmann, Phys. Rev. A 6, 1280 (1972); C. J. Borde, J. L. Hall, C. V. Kunasz, and D. G. Hummer, Phys. Rev. A 14, 236 (1976).
[19]B. Decomps, M. Dumont, and M. Ducloy, *Laser Spectroscopy of Atoms and Molecules* (Springer-Verlag, Berlin, 1976), p. 283.
[20]E. U. Condon and G. H. Shortley, *The Theory of Atomic Spectra* (University, Cambridge, 1959), p. 63.
[21]C. Wieman and T. Hänsch, Phys. Rev. Lett. 36, 1170 (1976).
[22]R. T. Menzies, Sci. Rep. No. 11-AF-AFOSR 68-1492, 1965 (unpublished).
[23]W. R. Bennett Jr., S. F. Jacobs, J. T. Latourette, and R. Rabinowitz, Appl. Phys. Lett. 5, 56 (1964).
[24]A. Le Floch, R. Le Naour, and G. Stephan, Opt. Commun. 20, 42 (1977).
[25]H. K. Holt, Phys. Rev. A 2, 233 (1970); P. R. Berman, Appl. Phys. 6, 283 (1975).
[26]B. D. Fried and S. D. Conte, *The Plasma Dispersion Function* (Academic, New York, 1961).
[27]C. V. Heer and R. D. Graft, Phys. Rev. 140, A1088 (1965).

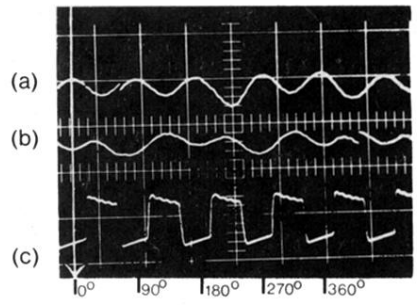

FIG. 5. Observation of the optical anisotropy induced by the saturating field. (a) Portion of the probe modulated at $4\omega_p$ (test tube switched on). (b) Portion of probe output modulated at $4\omega_p$ with the polarization of the laser field rotated by 90° as compared to preceding curve. This rotation has been obtained from a rotation by 45° of the $\frac{1}{2}\lambda_i$ plate. (c) Signal in phase with the rotation of the $\frac{1}{2}\lambda_e$ plate (one cycle corresponds to a rotation of 90°).